RNAi Targeting-STIL Suppresses Cell Growth and Induces Apoptosis of Lung Cancer NCI-H1299 Cells via Inactivation of Akt/SAPK/TAK1 Pathways

Hailong Li
Gansu University of Traditional Chinese Medicine https://orcid.org/0000-0002-5972-907X

Rong Niu
Department of external chest, Gansu Provincial Cancer Hospital, Lanzhou 730000, P. R. China

Yi Zhang
Clinical College of Traditional Chinese Medicine, Gansu University of Chinese Medicine, Lanzhou 730000, P. R. China

Yanmei Song
Department of internal medicine, First School of clinical Medicine, Gansu University of Chinese Medicine, Lanzhou 730000, P. R. China. 2Research Center of Traditional Chinese Medicine, Gansu Province, Lanzhou 730000, P. R. China

Jing Wang
Department of internal medicine, First School of clinical Medicine, Gansu University of Chinese Medicine, Lanzhou 730000, P. R. China. 2Research Center of Traditional Chinese Medicine, Gansu Province, Lanzhou 730000, P. R. China

Yali Yang
Department of internal medicine, First School of clinical Medicine, Gansu University of Chinese Medicine, Lanzhou 730000, P. R. China. 2Research Center of Traditional Chinese Medicine, Gansu Province, Lanzhou 730000, P. R. China

Yongqiang Duan
Research Center of Traditional Chinese Medicine, Gansu Province, Lanzhou 730000, P. R. China

Xiangdong Zhu
Research Center of Traditional Chinese Medicine, Gansu Province, Lanzhou 730000, P. R. China

Zhiming Zhang
Gansu cancer clinical medicine research center of integrated Traditional Chinese and Western Medicine, Lanzhou 730000, P. R. China.

Yonghua Hu (1076123533@qq.com)
Department of internal medicine, First School of clinical Medicine, Gansu University of Chinese Medicine, Lanzhou 730000, P. R. China. 5Gansu cancer clinical medicine research center of integrated Traditional Chinese and Western Medicine, Lanzhou 730000,

Research

Keywords: STIL, lung adenocarcinoma, antibody array, shRNA, apoptosis

Posted Date: February 5th, 2021

DOI: https://doi.org/10.21203/rs.3.rs-174463/v1

Abstract

Background: Gradually emerged studies demonstrated that SCL/TAL1 interrupting locus (STIL or SIL) is upregulated in multiple kinds of fatal tumors; at present, there is no clean understanding about the role of STIL in lung adenocarcinoma cells. This study aimed to discover the significance of STIL in lung adenocarcinoma, so as to find a potential gene target for diagnosis and therapy.

Methods: STIL expression in lung adenocarcinoma tissue and clinical pathological characteristic was analyzed using the online databases, UALCAN and GEPIA. Lentivirus STIL-shRNA was manufactured and transducted into lung adenocarcinoma cells to seek and analyze the effects on tumor phenotype. The cell proliferation was assessed using Cellomics Array Scan imaging assay, and colony-formation assay, respectively. The apoptosis was detected by flow cytometry assay. Moreover, the antibody array of PathScan Cancer Phenotype, PathScan stress and apoptosis pathway was used to explore relevant molecular mechanisms following STIL knockdown in NCI-H1299 cells.

Results: The clinical pathological characteristic assay showed that STIL is upregulated in lung adenocarcinoma tissues, and this trend was associated with cancer stage1 and histological subtypes. Silencing experiment showed that downregulation of STIL could inhibit cell growth and colony formation, induce cell apoptosis, and a G2 phase arrest effect significantly, and antibody array detection revealed that p-Bad were upregulated, and p-Akt, p-Bad, p-HSP27, p-SAPK/JNK, p-TAK1, Vimentin, CD45, PCNA and Ki-67 were downregulated significantly after STIL silenced in NCI-H1299 cells.

Conclusions: In conclusion, STIL is overexpressed in lung adenocarcinoma tissues compared with normal lung tissue. Knockdown of STIL could inhibit cell growth and colony formation ability, promote apoptosis via Akt/SAPK/TAK1 signal pathways inactivation.

Introduction

Lung cancer kept the record of the highest morbidity and mortality disease among a variety of malignant cancers in China [1]. As the most prevalent histological type of lung cancer, lung adenocarcinoma's relative survival rate of 5-year period increased with time, but not more than 21% [2]. Increasingly gene-targeted drugs against driver genes have been discovered and developed. However, gene targeted therapies against driver-gene-negative cases have not yet been fully developed. Efforts to identify a new potential target as drug for such cases are currently underway[3]. SCL/TAL1 interrupting locus (STIL or SIL), a centriolar assembly cytoplasmic protein, participate the processes of regulating the mitotic spindle checkpoint, the protein could be phosphorylated in mitosis and disappears when cell cycle enters G1 phase. It could interact with a mitotic regulatorand modulate Cdc2 kinase activity when spindle checkpoint was arrestted. Some experimental evidences come from published reports suggested that STIL is highly expressed in mutilple kinds of tumors accompanied by the features of increased mitotic activity[4], such as prostate cancer [5], pancreatic ductal adenocarcinoma [6] and lung cancer [7]. STIL could promote cellular proliferation, colony formation and suppress cellular apoptosis via affecting MAPK/ERK, PI3K/Akt and AMPK signaling pathways in prostate cancer [5]. SIL plays an essential role in the transition process from the G2 to the M phases of the cell cycle [4]. Silencing SIL in cancer cells could inhibited cell mitosis, decrease activation of the CDK1 (CDC2)-cyclin B complex, and even led to apoptosis in a p53-independent manner[7]. Inhibition of STIL enhances the efficacy of DNA damaging chemotherapeutic drugs significantly in the treatment of ovarian cancer[8].

In this current study, a lentivirus-short hairpin RNA (shRNA) containing STIL targeting sequences (Lv-shSTIL) was conceptualized and manufactured, and transduced into lung adenocarcinoma NCI-H1299 cells, to analyze the potential effects of silencing STIL on the phenotype of cancer. To be brief, a series of experiments including MTT, Cellomics Array Scan imaging, and colony formation assays were choosed to detect cell proliferation, and to analyze apoptosis and cell cycle were detected by flow cytometry assay. Besides this, the regulatory role of STIL in lung adenocarcinoma cells growth in vivo, two antibody PathScan arrays about cancer phenotype, stress and apoptosis were used to determine the underlying molecular mechanisms associated with STIL knockdown.

Materials And Methods

Extraction and analyzes of clinical data of STIL.

The clinical data about STIL expression in lung adenocarcinoma and clinical-pathological characteristic was collected using UALCAN[9] and GEPIA[10] web server (supported by TCGA database and the GTEx projects). STIL expression levels in lung adenocarcinoma tissues and adjacent tissues or Nodal Metastasis state were compared between lung adenocarcinoma tissues and adjacent tissues, and expressed as aberrant transcripts per million (TPM) values. Besides this, the correlation between STIL expression levels and prognosis in lung adenocarcinoma tissues were also analyzed by searching UALCAN, GEPIA and KM plotter [11]online database.

Cell lines and cell preparation

Lung cell line NCI-H1299 and 293T cell lines were provided by Genechem Company (Shanghai, China). All cell lines were kept in the medium composed of DMEM supplemented with 100 IU/mL Penicillin and 100 μg/mL Streptomycin, and 10% heat-inactivated fetal bovine serum (BSA: Zhejiang Tianhang Biotechnology Co. Ltd.) in a humidified cell incubator having an atmosphere of 5% CO_2 at 37℃. All cells reaching to exponential growth stage were used for further experiments.

Lentiviral infection of lung adenocarcinoma NCI-H1299 cells.

Human lung adenocarcinoma NCI-H1299 cells were seeded in plates with six-well at 5×10^4 cells/well and incubated at 37℃in 50 mL/L CO_2 until 30% confluence was reached. The study was designed as negative control group (shCtrl, transfected with empty green fluorescent protein (GFP) lentivirus) and shSTIL group (shSTIL, transfected with shSTIL GFP lentivirus). A sufficient amount of lentivirus was transfected into NCI-H1299 cells according to the multiplicity of infection (MOI) appropriately. The cells were repeatedly cultured in the culture medium. GFP-tagged gene expression was monitored under a fluorescence microscope at 3 d after transfection, and cells with the transfection efficiency more than 80% were selected for subsequent analysis. Cells were harvested at 48h after post-transfection to guarantee further analysis.

ShSTIL plasmid transfection in 293T cells.

The 293T cells at the logarithmic growth phase were seeded in 24-well plate with 5×10^4/mL until reached 80–90% confluence and the culture medium was changed with fresh medium by opti-MEM1 with 400 μL for RNAi plasmid transfection. Next, the successfully constructed plasmids containing shSTIL and shCtrl with 0.5μg and lipofectamine 2000 (Life Technologies, China headquarters of USA company, Shanghai, China) were dissolved in opti-MEM respectively and maintained at room temperature for 5 minutes, and then, the plasmids and lipofectamine 2000 were mixed and remained at room temperature for 20 minutes. Once finished that the above mentioned step, the mixture of plasmid DNA and Lipofectamine 2000 were added to 293T cells and cultured for 6–8 hours in incubator at 37℃, 5% CO_2 environment, and replaced with fresh complete culture medium containing 10% serum. The transfection rate was observed by fluorescence microscope detection after 24 hours transfection.

RT-qPCR analysis of knockdown efficiency in NCI-H1299 cells.

To detect the efficiency of silencing STIL in lung adenocarcinoma cells, the method of qPCR analysis was utilized. To be simple, lung adenocarcinoma cells at the exponential growth stage following successful silencing of STIL with lentivirus infection were collected and lysed for extracting total RNA using RNAiso Plus regent (Takara Bio, Dalian, China). The purity and concentration of extracted RNA were measured using P100 + UV-Vis spectrophotometer (Pultton, California, Sunnyvale, United States). Next, the reverse transcription reaction from to cDNA was performed using a Prime ScriptTM RT reagent Kit (Takara Bio, Dalian, China). Finally, the amplificationwas executed by a PCR Detection System (Roche, Light Cycle 9600, USA) using an SYBR Master Mixture (Yeasen, Shanghai, China), and the reaction of which was carried out in a final volume of 20 μL containing 1 μl of cDNA, 0.5 mM of each primer and 1X SYBR Master Mixture. The amplification reaction was operated as

the following programme: denaturation at 95°C for 15 sec, followed by 40 cycles of 95°C for 5 sec, 60°C for 30 sec, in which fluorescence was detected to catch the amplifid DNA. After completing the amplification procedure, the melting curve was created to analysis the specificity of the expected PCR product of STIL. The the amplified DNA of STIL were normalized to GAPDH to calculate the fold change using the tradition method $2^{-\Delta\Delta Ct}$. Each sample was run in triplicates for analysis. The primers used were as follows: STIL: forward, 5'- GAGTCAGATAATGGAATGATGGG – 3', reverse, 5'- CAGCAGTTGTCTTAGGGGAACA – 3'; GAPDH: forward, 5'- TGACTTCAACAGCGACACCCA – 3', reverse, 5'- CACCCTGTTGCTGTAGCCAAA – 3'.

Western blotting analysis of knockdown efficiency in 293T cells.

Following the transfection procedure for 36–48 hours, the 293T cells of both shSTIL and shCtrl groups were collected and washed twice using PBS solution, next, the collected 293T cells were lysed using ice-cold lysis buffer for 5 min for protein isolation. The total protein concentration of the collected 293T cells was detected with a protein assay kit (Bio-Rad Laboratories, Shanghai, China). The separation of protein samples was conducted using 10% SDS-PAGE, and the transference of which was conducted to PVDF membranes. The immunological blots were incubated with primary antibody (Mouse Anti-Flag, Sigma, 1:2000, China headquarters, Shanghai, China) in appropriate concentration at room temperature. following washed in 5% non-fat milk containing TBST saline at room temperature for 1 h, The immunological blots were incubated with the appropriate horseradish peroxidase (HRP)-conjugated secondary antibody (Goat Anti-Mouse IgG, 1:2000, Santa-Cruz Biotechnology, Dallas, Texas, USA) for 1.5 h. Finally, the bands were evaluated with a method of chemiluminescence (ECL, Thermo Scientific Pierce, Shanghai, China) and scanned images for quantification using ImageJ software (NIH Image for the Macintosh, USA). The western blotting experiments mentioned-above were performed in triplicate, and GAPDH (Mouse Anti-Flag, 1:2000, Santa-Cruz Biotechnology, Dallas, Texas, USA) was employed as a housekeeping control to normalize the expression of STIL protein expression by a semi-quantification method.

Cell proliferation detection by Cell counting with Cellomics Array detection.

The NCI-H1299 cells of both shSTIL and shCtrl groups were collected from plates using 0.25% trypsin-EDTA and suspended in standard medium until the cells grow to the logarithmic stage for cell counting with the cellomics array scan imaging detection. The specific procedures are as follows: the well prepared NCI-H1299 cells of both shSTIL and shCtrl groups were seeded in five wells at 1000 cells/well, followed by further incubation at 37 ℃ and 50 mL/L CO_2. A Cellomics Array Scan VT1 (Thermo Fisher Scientific) was utilized to monitor GFP expression of cells in both groups seeded in each well over 5 days continuously. In this study, statistical data of cells growth were mapped and cell proliferation curves were drawn to compare the multiplication ability of NCI-H1299 cells in both shSTIL and shCtrl groups.

Apoptosis assay.

The NCI-H1299 cells were harvested with 0.25% trypsin from and washed once with 4°C ice-cold D-Hanks (pH = 7.2 ~ 7.4) for centrifuge operation with the centrifuge force at 1300 rmp for 5 min. After rewashed with 1×binding buffer, the NCI-H1299 cells received another centrifuge operation at 1300 rmp for 3 min. Next, the NCI-H1299 Cells were resuspended in 200 μL binding buffer 10^6 cells/mL to execute apoptosis assay using a Annexin V-APC Apoptosis Detection Kit (MultiSciences, Hangzhou, China). The cell suspension of 100 μL volume was mixed with 10 μL Annexin V-APC for incubation in the dark for 15 min at room temperature. As a necessary step, a volume of 400–800μL 1×binding buffer was added to stained cells in proportion to the amounts of cells. The percentage of apoptotic rate was analyzed by flow cytometry in triplicate.

Caspase 3/7 activity assay.

Human lung adenocarcinoma NCI-H1299 cells were treated as a resuspended solution and seeded in 96-well plates in triplicate with a cell density of 1,000 cells/well at 37°C under incubation environment with 5% CO_2 for caspase 3/7 activity assay. Caspase 3/7 activity was then tested using a Caspase Glo 3/7 Assay (Promega Corporation, G8091, WI, USA) kit based on the manufacturer's protocol. The Caspase-Glo3/7 buffer solution and Caspase-Glo3/7 freeze-dried powder were

placed at 18–22 ℃ (room temperature) for balance. Then a volume of 10 mL Caspase-Glo3/7 buffer solution was added to the brown bottle containing the Caspase-Glo3/7 substrate, and the brown bottle was whirled or reversed repeatedly until the substrate completely dissolved to form the Caspase-Glo reaction solution. After cell counting, the cell suspension concentration was adjusted to 1 × 10^4 cells / well at room temperature, and a volume of 100 μL of non-negative control cells were added to the new 96 well plates per well. At the same time, a group of empty control group without cells was setted up (adding only 100 μL per well medium). Next, a volume of 100 μL Caspase-Glo reaction solution was added to each well. The culture plate was place with cells on the plate shaker and shake lightly for 30 minutes at 300–500 rpm speed. Then the cells were incubated at 18–22 ℃ for 2 hours. Absorbance values were measured with a microplate reader (SpectraMax i3X, MOLECULAR, California, USA) at 405 nm.

Cell cycle analysis by flow cytometry.

When the NCI-H1299 cells reached 80% confluence in the 6 cm dish of each experimental group, it will be resuspended in triplicate in full culture medium. For suspension cells, the supernatant was directly collected by centrifugation at 1300 rmp for 5 min, and then washed with the precooled D-Hanks (pH = 7.2 ~ 7.4) at 4 ℃. Next, the cells were treated with centrifuge operation at 1300 rmp for 5 min. and then treated with precooled 75% ethanol at 4 ℃ for at least 1 h. After removing the immobilization solution and the cells were washed using precooled D-Hanks, a certain volume (0.6-1 mL) of cell staining (composed with 40 × PI mother liquor (2 mg/mL), 100 × RNase mother liquor (10 mg/mL) and 1 × D-Hanks, and the proportion of which is 25: 10: 1000) solution was added to heavy suspension to stain cells with propidium iodide for cell cycle analysis according to cell quantity. The cell cycle detection was conducted using a Guava EasyCyte Plus Flow Cytometry System (Merck Millipore, Billerica, MA, USA).

Antibody Array assay of Cancer Phenotype,Stress and Apoptosis pathway.

To explore the activation of possible intracellular signaling related to the influences in lung adenocarcinoma caused by STIL silencing, the PathScan of Cancer Phenotype Antibody Array Kit (#14821, Cell Signaling Technology, Danvers, MA, USA), Stress and Apoptosis Signaling Antibody Array Kit (#12923, Cell Signaling Technology, Danvers, MA, USA) were used to screen and analysis potential proteins. After, till cells reaching around 85% confluence following lentivirus infection for 5 days, NCI-H1299 cells of both groups were collected and lysed to carry out detection in compliance with the manufacturer's instructions. The detection of cells between STIL silenced group and ShCtrl group was repeated in triplicate. Images were captured by exposing the slide to chemiluminescent film according to standard protocol.

Statistical analysis.

ALL data were expressed as the means ± standard deviation from at least 3 independent experiments. Statistical analyses were calculated with the method of Student’s two-tailed t-test. Differences with P values of < 0.05 are regarded as significant statistically.

Results

STIL was overexpressed in lung adenocarcinoma tissue with clinical features.

In order to understand the role of STIL lung adenocarcinoma tissues, and even find its potential clinical significances, we preliminarily analyzed the aberrant expression levels of STIL between lung adenocarcinoma tissues and adjacent tissues by searching and analyzing UALCAN and GEPIA web server which was based on TCGA datasets. This result showed that STIL is upregulated in lung adenocarcinoma tissues when comparing with adjacent normal tissues (Fig. 1(A, B)). Besides, the expression of STIL in Nodal Metastasis tissues, such as N0, N1, N2 lymph nodes was higher than that in normal tissues which embodied as Nodal Metastasis tissues having higher TPM values than normal tissues (Fig. 1C). The survival period of STIL overexpression group was less time than that in STIL lower expression group that was supported by UALCAN(Fig. 1D), GEPIA(Fig. 1E) and KM plotter online database(Fig. 1F). Summarily, STIL is upregulated in lung adenocarcinoma tissues, and

which was correlated with cancer nodal metastasis statues, such as N0, N1, N2. The survival period of STIL overexpression group was associated with less survival time.

ShRNA-mediated STILsilencing efficiency in NCI-H1299 cells and 293T cells.

To investigate the loss of functional role of STIL, the lung adenocarcinoma cell NCI-H1299 was cultured and successfully infected with Lv-shSTIL or Lv-shCtrl with an infection rate greater than 80% for up to 72 hours since lentivirus infection completed(Fig. 2(A, B)). The mRNA expression level of STIL was significantly decreased in Lv-shSTIL groups with significant knockdown efficiency amounts to 59% compared with Lv-shCtrl group ($P = 0.05$, Fig. 2C). Human embryonic kidney 293T cells were transfected with shSTIL plasmid or shCtrl plasmid, STIL protein expression was significantly decreased in the Lv-shSTIL group in 293T cells, respectively (Fig. 2(D, E)). The results showed STIL-shRNA could knockdown STIL expression of the target sequence effectively.

STIL silencing inhibited lung adenocarcinoma cell proliferation by Cellomics detection.

GFP-based Cellomics Array Scan imaging assay showed that the proliferation of NCI-H1299 cells was significantly inhibited in STIL-shRNA group relative to that of the Lv-shCtrl group. The number of NCI-H1299 cells and the fold-change of proliferation were significantly reduced in the STIL-shRNA-silenced lung adenocarcinoma cells on the third, fourth and fifth day following STIL silencing significantly completed in NCI-H1299 cells ($P < 0.001$, Fig. 3(A, B, C)). Consequently, the results suggested that knowdown of STIL could inhibit lung adenocarcinoma cell proliferation.

STIL silencing induced cell apoptosis.

To elucidate whether the silencing of STIL could induce apoptosis in NCI-H1299 cells further, apoptosis detection was designed to investigate the apoptotic rate between STIL silenced NCI-H1299 cells and negative control cells further. The apoptotic rate was assessed by flow cytometry using an Annexin V-APC Apoptosis Detection Kit. The proportion of apoptotic cells in NCI-H1299-silenced cells was significantly higher than that in the control cells ($P < 0.001$, Fig. 4(A, B)). These data suggested that the silencing of STIL could affect cell survival and induce apoptosis.

Silencing STIL induced elevation of Caspase 3/7 activity.

The caspase 3/7 activity of Lv-shSTIL group was calculated based on the Lv-shCtrl group. Compared with Lv-shCtrl group, the caspase 3/7 activity increased in the Lv-shSTIL group, indicating that the number of apoptotic cells in Lv-shSTIL group increased significantly ($P < 0.001$, Fig. 4C), reflecting STIL silencing could induce cell apoptosis in NCI-H1299 cells.

Silencing STIL induced cell cycle arrest at the G2/M stage.

To elucidate whether the silencing of STIL could arrest the cell cycle in NCI-H1299 cells further. The cell cycle was assessed between STIL silenced NCI-H1299 cells and shCtrl group cells by flow cytometry using PI (Sigma, USA). Three days after shRNA lentivirus infection, there was no significant difference in G1 cells in the experimental group. The number of NCI-H1299-silenced cells in the S phase decreased, and the number of cells in the G2/M phase increased than that in shCtrl group cells ($P < 0.05$), as shown in Fig. 4(D, E). These data suggested that the silencing of STIL could arrest the cell cycle in G2 phase.

STIL silencing induces molecular alterations in cancer phenotype and apoptosis.

To investigate the adjustment mechanisms of STIL played in the tumorigenesis of lung adenocarcinoma, PathScan of Cancer Phenotype, Stress and Apoptosis Signaling Antibody Array were employed to analysis aberrantly expressed proteins in NCI-H1299 cells after STIL knockdown. The results demonstrated that knockdown of STIL significantly induced downregulation of phosphorylation expression of p-Akt,p-Bad□p-HSP27□p-SAPK/JNK, p-TAK1, Vimentin, CD45, PCNA and Ki-67 at the levels about − 24.82%, 17.09%, -23.93%, -21.75%, -11.07%, -17.19%, -26.43%, -20.46% and − 16.36%, respectively (p

value = 0.0000, 0.0038, 0.0027, 0.0079, 0.0458, 0.0416, 0.0430, 0.0024 and 0.0002), as shown in Fig. 5 (A, B, C) and Fig. 6 (A, B, C), & Table 1, 2. This result indicated that STIL silencing could suppress cell proliferation and induce apoptosis reflected from the downregulation of these molecules, such as Vimentin, CD45, PCNA and Ki-67, and the process of which was probably via inactivation of p-Akt/p-SAPK//p-TAK1 pathway in lung adenocarcinoma cells. Certainly, we can conclude from the results that phosphorylation of p-Akt□p-Bad□p-HSP27□p-SAPK/JNK and p-TAK1 play important roles in the tumorigenesis process and maintenance of cancerous phenotype of NCI-H1299 cells. Furthermore, insightful studies are needed to clarify the mechanisms of STIL in lung adenocarcinoma progression.

Discussion

In this study, we performed clinical data analysis of STIL in lung adenocarcinoma tissues compared with normal tissues to discover its expression and clinical significances by searching and extracting from the data supported by UALCAN and GEPIA web server. It has been confirmed that STIL is upregulated in lung adenocarcinoma tissues, and its overexpression was associated with cancer metastasis, besides, overexpression of STIL would result in a poor prognosis with less survival time. In summary, it is suggested that overexpression of STIL might act as a potential lung adenocarcinoma biomarker that was related to lymph node metastasis and vicious prognosis with less survival time. Therefore, it is promising if STIL would be chosen as new biomarker to attach importance to its role, function and relevant mechanisms.

In the present study, silencing STIL inhibited lung adenocarcinoma cell proliferation, reduced cell colony formation. Caspase 3/7 activity assay and apoptosis assay by flow cytometry showed that silencing STIL could induce lung adenocarcinoma cell apoptosis; cell cycle analysis by flow cytometry showed that silencing STIL could induce cell arrest at the G2 phase. These completed data demonstrated that STIL overexpression plays an essential role in lung adenocarcinoma tumorigenicity. It is suggested that STIL contributes to the pathogenesis of lung adenocarcinoma and STIL overexpression may be an early event in lung adenocarcinoma carcinogenesis. Therefore, STIL may represent a new promising target for gene therapy of lung adenocarcinoma.

The results were coincident with the reports that STIL knochdown could suppress cell growth through apoptosis and cell cycle arrest [4–6, 8]. Apoptosis has been proved as a principal strategy, and there are multiple signaling pathways involved in the process of apoptosis. However, the mechanisms of apoptosis induced by STIL silencing still kept unclear. Therefore, the Stress and Apoptosis Signaling Antibody Array and Cancer Phenotype Antibody assay were employed to detect relevant molecular alterations about apoptosis and cancer phenotype comprehensively. The two pathways and targets included in these two arrays made it easier to screen and analyze relevant mechanisms of apoptosis. Previous reports demonstrate that these kinds of arrays have been used to detect mechanisms molecular in multiple cancers, such as in glioblastoma[12], gastric cancer[13] and esophageal squamous carcinoma[14]. In the present study, the completed results of PathScan Stress and Apoptosis Signaling Antibody array assay showed that STIL silencing could inhibit the activation of phosphorylation level of p-Akt, p-Bad, p-HSP27,p-SAPK/JNK and p-TAK1 which could reflect molecule alterations during apoptosis. The results of the PathScan of Cancer Phenotype assay showed that STIL knockdown could block the activation of Vimentin, CD45, PCNA, and Ki-67which represent essential molecules in cancer phenotype change.

Vimentin, a major constituent of the intermediate filament family of proteins, is overexpressed in various epithelial cancers including lung cancer, and the overexpression of which in cancer was associated with tumorigenesis features, such as, accelerated tumor growth, invasion [15] TNM stage, lymph node metastasis and unfavourable prognosis [16]. Vimentin was verified as an independent prognostic factor regarding the overall survival time of gastric cancer [17]. CD45, also known as protein tyrosine phosphatase receptor type C, abbreviated as PTPRC, belongs to the protein tyrosine phosphatase (PTP) family. Reports showed that overexpression of CD45 was associated with weak treatment response and adverse survival profiles in elderly patients with acute myeloid leukemia [18]. Increased intraepithelial CD45RO + TILs was an independent positive prognostic factor for disease-specific survival in all patients and squamous cell carcinoma [19]. The CD45 + erythroid progenitor cells (CD45 + EPC) played an immunosuppressive role in the responses of the impaired T cell commonly appeared

in patients with advanced cancer, and the mechanism of which could be ascribed in that reactive oxygen species production contributed to CD45 + EPC-mediated immunosuppression[20]. CD45RO is a nucleus-located cofactor of DNA polymerase delta which participates in the RAD6-dependent DNA repair pathway when coming across DNA damage [21]. Antigen Ki-67, a nuclear protein, which is relevant with ribosomal RNA transcription and responsible for cellular proliferation. The activated antigen Ki-67 would inhibit the progress of ribosomal RNA synthesis, and Antigen Ki-67 could increase markedly during cell progression through S phase in the cell cycle. A report showed that the expression of Ki-67 in lung adenocarcinoma tissue is associated with poor tumor differentiation, and negatively affects patients' survival in advanced-stage lung cancer [22]. It has been proved that Ki-67 is a valuable predictive factor because overexpression of it was associated with lymph node metastasis and advanced TNM stages [23]. The overexpression of p-AKT was related to DNA aneuploidy which acts as a useful marker in a number of gastric cancer cases [24]. The survival time of PI3K and p-Akt-positive expression was significantly reduced in advanced NSCLC patients, and the overexpression of p-Akt was considered as an independent prognosis marker of poor outcome in advanced NSCLC[25]. AKT plays an essential role in the PI3K/Akt signaling pathway in cancer cells, and p-AKT, an activated form of AKT, plays avital role in the cell survival mechanisms and signal transduction pathways concerning tumorigenesis [26]. AKT activation which was caused by the production of PIP3 by PI3K, and PTEN dephosphorylates PIP3 at the 3' position, would give rise to the activation of downstream apoptosis signaling pathways which leads to apoptosis in the end[27]. Cell apoptosis would be induced by BAD and forkhead transcription factor (FKHR-L1) direct phosphorylation, and which could reduce the stress-activated protein kinase/c-Jun N-terminal kinase (SAP/JNK) signaling pathway that could be activated by extracellular proinflammatory cytokines or physical stress and turned into phosphorylated SAPK/JNK (p-SAPK/JNK). TAK1, also known as MAP3K7(its full name is mitogen-activated protein kinase kinase kinase 7), participates a variety of transcription regulation including apoptosis. Once, activated and turned into phosphorylated p-TAK1, it could also phosphorylate and activate MAPKKs which could bring about activation of MAPKs such as ERK, p38, and JNK[28]. Phosphorylation of TAK1 at Ser412 site contributes to the activation of NF-κB signaling and boosts aggressiveness in ovarian cancer cells, inhibition of TAK1 activity dramatically impairs tumor growth and metastasis in ovarian cancer [29]. In this study, p-TAK1 was downregulated in STIL silenced NCI-H1299 cells compared with negative control NCI-H1299 cells. These data suggested that the mechanisms of growth inhibition and apoptosis effects induced by STIL silencing are associated with the inactivation of phosphorylation expression of p-Akt, p-Bad, p-HSP27, p-SAPK/JNK, p-TAK1, Vimentin, CD45, PCNA and Ki-67.

Collectively, STIL is upregulated in lung adenocarcinoma tissues compared with normal lung tissue. Knockdown of STIL could inhibit lung adenocarcinoma cell growth and colony formation ability, promote apoptosis, and the mechanisms of which may block the phosphorylation of p-Akt/p-SAPK/p-TAK1 signal pathway and reverse the expressions of cancerous phenotype markers. Therefore, STIL may be considered as a promising and valuable target for gene therapy strategy in the treatment of lung adenocarcinoma.

Abbreviations

STIL: SCL/TAL1 interrupting locus; TPM: transcripts per million; shRNA: short hairpin RNA.

Declarations

Ethics approval and consent to participate

Consent publication

The authors all agreed for publication of this paper.

Availability of data and material

All data and materials generated and analyzed during the present study are available from the corresponding author on reasonable request.

Competing interests

The authors declare that they have no competing interests in this paper.

Funding

This program was support by the University Research Project of Gansu Province (2018A-049 and 2017A-212); The Foundation of Natural Science of Gansu Province (20JR5RA189); the Foundation of Innovation ability improvement project of colleges and universities in Gansu Province (2019A-075). All authors declared that we have no conflict of interest in this paper.

Authors' Contributions

(I) Conception and design: Hailong Li, Rong Niu, Yonghua Hu, Zhiming Zhang; (II) Administrative support: no; (III) Provision of study materials or patients: Hailong Li, Yongqiang Duan, Yi Zhang, Xiangdong Zhu; (IV) Collection and assembly of data: Yonghua Hu, Yi Zhang, Yanmei Song, Jing Wang, Yali Yang; (V) Data analysis and interpretation: Hailong Li, Yonghua Hu, Xiangdong Zhu; (VI) Manuscript writing: All authors; (VII) Final approval of manuscript: All authors. The authors declare that they have no competing interests in this paper.

Acknowledgments

This program was supported by the University Research Project of Gansu Province (2018A-049); The Foundation of Natural Science of Gansu Province (20JR5RA189 and 17JR5RA169); the Foundation of Innovation ability improvement project of colleges and universities in Gansu Province (2019A-075), the Planned projects of Department of science and technology of Gansu Province (18JR2FA001). All authors declared that we have no conflict of interest in this paper.

References

1. Chen W, Zheng R, Baade PD, et al: Cancer statistics in China, 2015. CA Cancer J Clin 66:115-32, 2016
2. Lu T, Yang X, Huang Y, et al: Trends in the incidence, treatment, and survival of patients with lung cancer in the last four decades. Cancer Manag Res 11:943-953, 2019
3. Saito M, Suzuki H, Kono K, et al: Treatment of lung adenocarcinoma by molecular-targeted therapy and immunotherapy. Surgery Today 48:1-8, 2017
4. Erez A, Castiel A, Trakhtenbrot L, et al: The SIL gene is essential for mitotic entry and survival of cancer cells. Cancer Res 67:4022-7, 2007
5. Wu X, Xiao Y, Yan W, et al: The human oncogene SCL/TAL1 interrupting locus (STIL) promotes tumor growth through MAPK/ERK, PI3K/Akt and AMPK pathways in prostate cancer. Gene 686:220-227, 2019
6. Kasai K, Inaguma S, Yoneyama A, et al: SCL/TAL1 interrupting locus derepresses GLI1 from the negative control of suppressor-of-fused in pancreatic cancer cell. Cancer Res 68:7723-9, 2008
7. Erez A, Perelman M, Hewitt SM, et al: Sil overexpression in lung cancer characterizes tumors with increased mitotic activity. Oncogene 23:5371-7, 2004
8. Rabinowicz N, Mangala LS, Brown KR, et al: Targeting the centriolar replication factor STIL synergizes with DNA damaging agents for treatment of ovarian cancer. Oncotarget 8:27380-27392, 2017
9. Chandrashekar DS, Bashel B, Balasubramanya SAH, et al: UALCAN: A Portal for Facilitating Tumor Subgroup Gene Expression and Survival Analyses. Neoplasia 19:649-658, 2017

10. Tang Z, Li C, Kang B, et al: GEPIA: a web server for cancer and normal gene expression profiling and interactive analyses. Nucleic Acids Research:W1, 2017
11. Gyorffy B, Surowiak P, Budczies J, et al: Online survival analysis software to assess the prognostic value of biomarkers using transcriptomic data in non-small-cell lung cancer. PLoS One 8:e82241, 2013
12. Li J, Ren S, Liu Y, et al: Knockdown of NUPR1 inhibits the proliferation of glioblastoma cells via ERK1/2, p38 MAPK and caspase-3. Journal of Neuro-Oncology 132:15-26, 2017
13. Li H, Song Y-H, Du Z-P, et al: COPB2-shRNA suppresses cell growth and induces apoptosis of STAD SGC-7901 cells via inactivation of p38 MAPK/Smad2/Chk1/2 as an oncogene. Translational Cancer Research 7:1714-1727, 2018
14. Li B, Li YM, He WT, et al: Knockdown of DDX46 inhibits proliferation and induces apoptosis in esophageal squamous cell carcinoma cells. Oncology Reports 36:223, 2016
15. Satelli A, Li S: Vimentin in cancer and its potential as a molecular target for cancer therapy. Cell Mol Life Sci 68:3033-46, 2011
16. Yin S, Chen FF, Yang GF: Vimentin immunohistochemical expression as a prognostic factor in gastric cancer: A meta-analysis. Pathol Res Pract 214:1376-1380, 2018
17. Wang JY, Wu T, Ma W, et al: Expression and clinical significance of autophagic protein LC3B and EMT markers in gastric cancer. Cancer Manag Res 10:1479-1486, 2018
18. Guo L, Chen L, Wang H: CD45 correlates with adverse risk stratification, decreased treatment response and unfavorable survival profiles in elderly acute myeloid leukemia patients. Cancer Biomark 23:455-463, 2018
19. Kilvaer TK, Paulsen EE, Khanehkenari MR, et al: The presence of intraepithelial CD45RO+ cells in resected lymph nodes with metastases from NSCLC patients is an independent predictor of disease-specific survival. Br J Cancer 114:1145-51, 2016
20. Zhao L, He R, Long H, et al: Late-stage tumors induce anemia and immunosuppressive extramedullary erythroid progenitor cells. Nat Med 24:1536-1544, 2018
21. Association analysis of CD45RO expression in lung adenocarcinoma with clinicopathological features and survival rate. Journal of Chinese Medical University 47:448-453, 2018
22. Kim CH, Lee HS, Park JH, et al: Prognostic role of p53 and Ki-67 immunohistochemical expression in patients with surgically resected lung adenocarcinoma: a retrospective study. J Thorac Dis 7:822-33, 2015
23. Wei DM, Chen WJ, Meng RM, et al: Augmented expression of Ki-67 is correlated with clinicopathological characteristics and prognosis for lung cancer patients: an up-dated systematic review and meta-analysis with 108 studies and 14,732 patients. Respir Res 19:150, 2018
24. Hisamatsu Y, Oki E, Otsu H, et al: Effect of EGFR and p-AKT Overexpression on Chromosomal Instability in Gastric Cancer. Ann Surg Oncol 23:1986-92, 2016
25. Jiang AG, Yu H, Huang JA: Expression and clinical significance of the phosphatidylinositol 3-kinase/protein kinase B signal transduction pathway in non-small cell lung carcinoma. Oncol Lett 8:601-607, 2014
26. Martini M, De Santis MC, Braccini L, et al: PI3K/AKT signaling pathway and cancer: an updated review. Annals of Medicine 46:372-383
27. Lu XX, Cao LY, Chen X, et al: PTEN Inhibits Cell Proliferation, Promotes Cell Apoptosis, and Induces Cell Cycle Arrest via Downregulating the PI3K/AKT/hTERT Pathway in Lung Adenocarcinoma A549 Cells. Biomed Res Int 2016:2476842, 2016
28. Mihaly SR, Ninomiya-Tsuji J, Morioka S: TAK1 control of cell death. Cell Death Differ 21:1667-76, 2014
29. Cai PC, Shi L, Liu VW, et al: Elevated TAK1 augments tumor growth and metastatic capacities of ovarian cancer cells through activation of NF-kappaB signaling. Oncotarget 5:7549-62, 2014

Tables

Table 1
Detected proteins screened and validated by PathScan® of cancer phenotype array between shCtrl-infected cells and shSTIL-infected cells.

	Target	Site	Modification	Gray Value (AVERAGE ± STDEV)		P VALUE	Up/Down
				shCtrl	shSTIL		
1	Positive Control	N/A	N/A	\	\	\	\
2	Negative Control	N/A	N/A	\	\	\	\
3	CD31 (PECAM-1)	N/A	N/A	17.23 ± 5.02	14.52 ± 1.57	0.2527	-15.76%
4	EpCAM	N/A	N/A	16.93 ± 5.82	13.32 ± 1.54	0.1941	-21.36%
5	Vimentin	N/A	N/A	23.37 ± 3.63	19.35 ± 1.25	0.0416	-17.19%
6	CD44	N/A	N/A	60.80 ± 6.49	55.70 ± 3.19	0.1147	-8.39%
7	CD45	N/A	N/A	19.55 ± 5.08	14.38 ± 2.02	0.0430	-26.43%
8	PCNA	N/A	N/A	55.65 ± 5.42	44.27 ± 4.30	0.0024	-20.46%
9	Ki-67	N/A	N/A	99.10 ± 3.08	82.88 ± 6.29	0.0002	-16.36%
10	p27 Kip1	N/A	N/A	99.30 ± 8.47	98.32 ± 3.67	0.7995	-0.99%
11	E-Cadherin	N/A	N/A	16.98 ± 6.45	15.95 ± 1.44	0.7161	-6.08%
12	N-Cadherin	N/A	N/A	90.85 ± 6.71	88.63 ± 2.22	0.4708	-2.44%
13	VE-Cadherin	N/A	N/A	29.00 ± 8.09	23.95 ± 2.82	0.1976	-17.41%
14	MUC1	N/A	N/A	23.52 ± 4.95	18.90 ± 3.87	0.1019	-19.63%
15	p-Rb	Ser807/811	Phosphorylation	100.20 ± 5.71	103.43 ± 1.32	0.2289	3.23%
16	HIF-1a	Total	N/A	17.02 ± 2.70	14.43 ± 1.80	0.0796	-15.18%
17	Survivin	Total	N/A	49.55 ± 4.20	52.07 ± 3.79	0.0904	6.19%
18	p53	Total	N/A	9.95 ± 2.47	11.27 ± 1.70	0.3080	13.23%
19	HER2/ErbB2	Total	N/A	9.70 ± 0.82	8.87 ± 1.24	0.1998	-8.59%
20	Met	Total	N/A	25.53 ± 1.53	26.97 ± 2.07	0.2031	5.61%
21	EGF Receptor	Total	N/A	14.38 ± 1.23	14.08 ± 1.37	0.6984	-2.09%

Notes: The results indicated that knockdown of STIL could significantly induce downregulation of phosphorylation of 5 targets in the Stress and Apoptosis Signaling pathway, including Vimentin,CD45□PCNA□Ki-67 at different levels.

Table 2
Detected proteins screened and validated by PathScan® of Stress and Apoptosis Signaling Antibody array between shCtrl-infected cells and shSTIL-infected cells.

	Target	Site	Modification	Gray Value (AVERAGE ± STDEV)		P VALUE	Up/Down
				shCtrl	shSTIL		
1	Positive Control	N/A	N/A	\	\	\	\
2	Negative Control	N/A	N/A	\	\	\	\
3	p-ERK1/2	Thr202/Try204	Phosphorylation	25.32 ± 6.29	24.12 ± 3.74	0.6965	-4.74%
4	p-Akt	Ser473	Phosphorylation	36.67 ± 1.80	27.57 ± 2.27	0.0000	-24.82%
5	p-Bad	Ser136	Phosphorylation	85.22 ± 8.52	99.78 ± 4.27	0.0038	17.09%
6	p-HSP27	Ser82	Phosphorylation	36.22 ± 4.96	27.55 ± 2.04	0.0027	-23.93%
7	p-Smad2	Ser465	Phosphorylation	25.48 ± 4.10	22.50 ± 1.87	0.1359	-11.71%
8	p-p53	Ser15	Phosphorylation	13.20 ± 6.21	12.17 ± 4.53	0.7486	-7.83%
9	p-p38 MAPK	Thr180/Try182	Phosphorylation	21.03 ± 4.80	19.88 ± 3.28	0.6383	-5.47%
10	p-SAPK/JNK	Thr183/Try185	Phosphorylation	34.87 ± 3.94	27.28 ± 4.00	0.0079	-21.75%
11	cleaved PARP	Asp214	Cleavage	22.28 ± 7.37	20.25 ± 5.58	0.6018	-9.12%
12	cleaved Caspase-3	Asp175	Cleavage	26.13 ± 6.54	25.25 ± 2.50	0.7636	-3.38%
13	cleaved Caspase-7	Asp198	Cleavage	29.43 ± 7.80	25.13 ± 1.72	0.2395	-14.61%
14	IkBa	Total	N/A	87.37 ± 8.61	85.30 ± 6.31	0.6455	-2.37%
15	p-Chk1	Ser345	Phosphorylation	35.55 ± 7.50	29.20 ± 2.29	0.0952	-17.86%
16	p-Chk2	Thr68	Phosphorylation	48.45 ± 9.11	43.75 ± 3.57	0.2665	-9.70%
17	p-IkBa	Ser32/36	Phosphorylation	33.05 ± 5.92	31.63 ± 4.26	0.6442	-4.29%
18	p-eIF2a	Ser51	Phosphorylation	24.47 ± 7.24	20.63 ± 3.35	0.2665	-15.67%

Notes: The results indicated that knockdown of STIL could significantly induce downregulation of phosphorylation of 5 targets in the Stress and Apoptosis Signaling pathway, including p-Akt,p-Bad□p-HSP27□p-SAPK/JNK□p-TAK1at different levels.

	Target	Site	Modification	Gray Value (AVERAGE ± STDEV)		P VALUE	Up/Down
				shCtrl	shSTIL		
19	p-TAK1	Ser412	Phosphorylation	82.63 ± 9.01	73.48 ± 3.93	0.0458	-11.07%
20	Survivin	Total	N/A	88.08 ± 6.27	93.53 ± 3.38	0.0904	6.19%
21	a-Tubulin	Total	N/A	40.73 ± 8.13	33.37 ± 4.36	0.0791	-18.09%

Notes: The results indicated that knockdown of STIL could significantly induce downregulation of phosphorylation of 5 targets in the Stress and Apoptosis Signaling pathway, including p-Akt,p-Bad□p-HSP27□p-SAPK/JNK□p-TAK1at different levels.

Figures

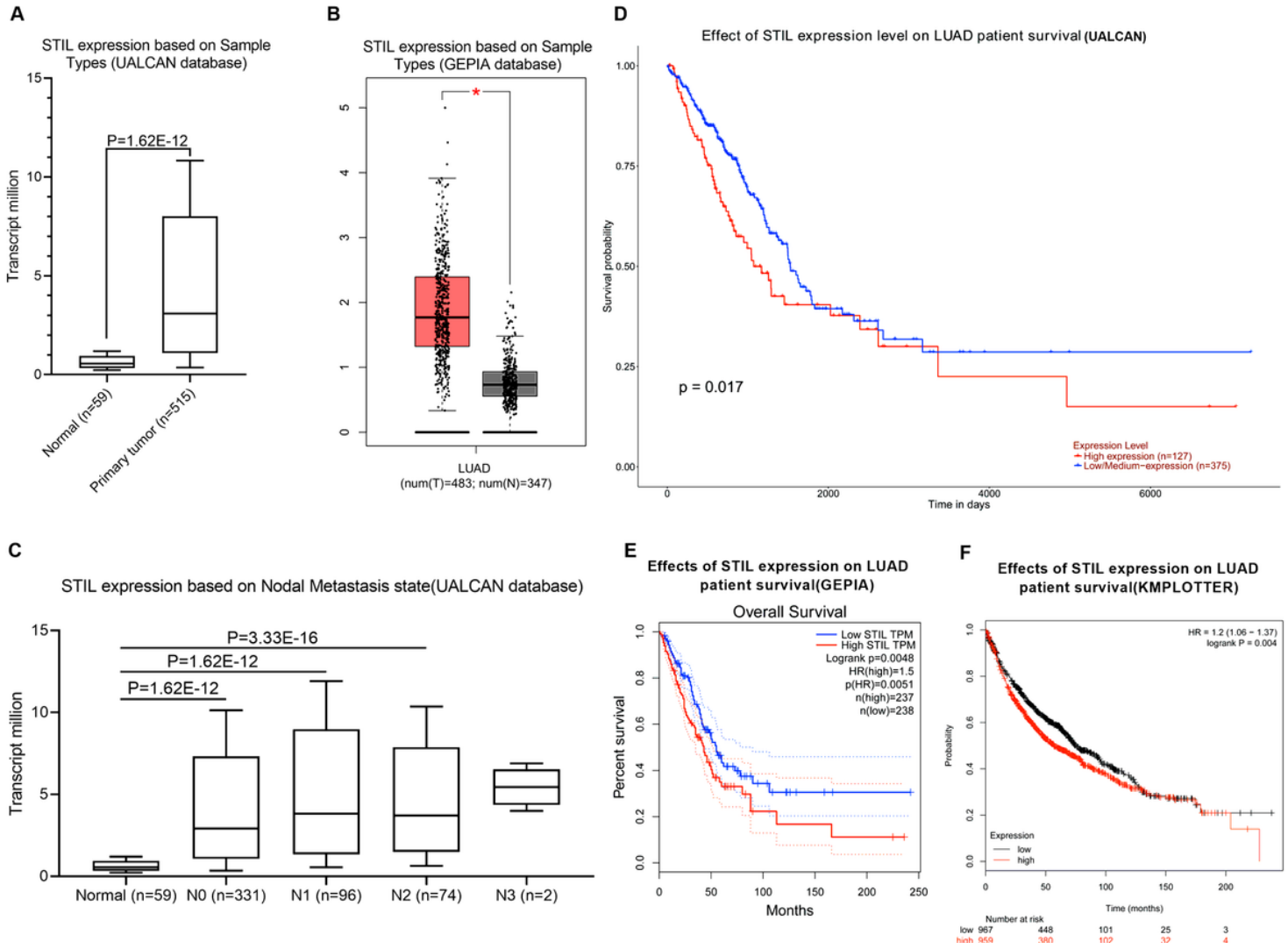

Figure 1

Expression of STIL in lung adenocarcinoma tissues and clinical features. Expression of STIL were upregulated in tumors than in corresponding adjacent tissues of lung, the median value of lung adenocarcinoma tissues and corresponding

adjacent tissues were 73.973 and 35.160respectively, and Log2 fold change was 1.052, as shown is the value of lung adenocarcinoma in (Figure 1A, B) (GEPIA database supported by Match TCGA normal and GTEx data). Overexpression of STIL in cancer stage1, 2, 3, 4 embodies more TPM values than normal tissues (Figure 1C) supported by both UALCAN and GEPIA web server. Overexpression of STIL in tumor stage1 embodies higher TPM value than in normal tissues (Figure 1C). The survival period of STIL overexpression group was less time than that in STIL lower expression group that was supported by UALCAN (Figure 1D), GEPIA (Figure 1E) and KM plotter online database (Figure 1F). Summarily, STIL is upregulated in lung adenocarcinoma tissues, and which was correlated with cancer nodal metastasis statues, such as N0, N1, N2. The survival period of STIL overexpression group was associated with less survival time.

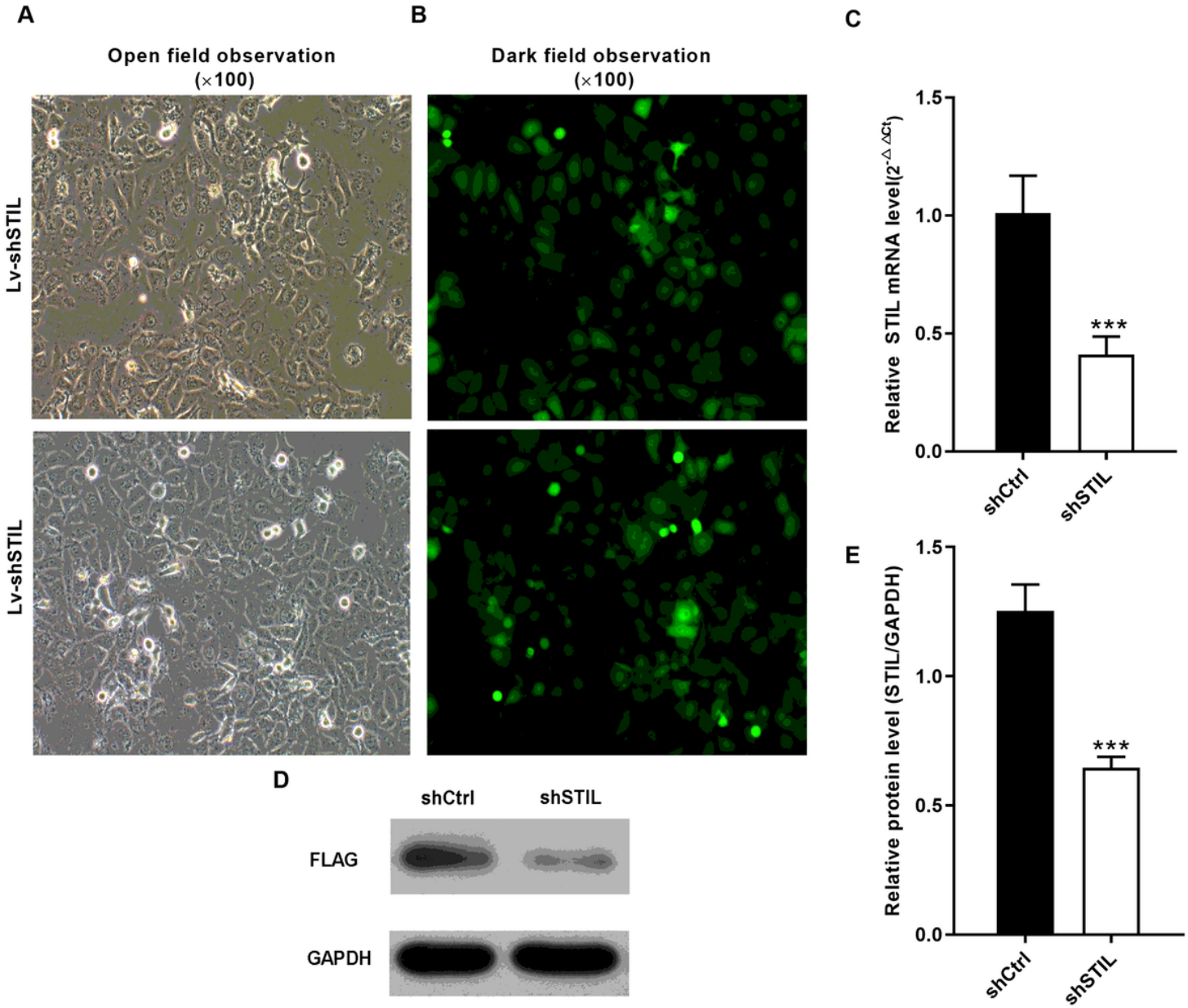

Figure 2

(A, B, C, D): Effect of STIL infection efficiency and gene knockdown efficiency in NCI-H1299 cells and 293T cells. The mRNA expression level of STIL were significantly downregulated ($p < 0.01$) in Lv-shSTIL group, compared with Lv-shCtrl group with a significant knockdown efficiency amounts to 78.9% ($p < 0.01$), as shown in Figure 3(A). Human embryonic kidney 293T cells were infected with STIL-shRNA lentivirus or negative control lentivirus, as shown in Figure 3(A), STIL mRNA and protein expression were greatly reduced in the STIL-shRNA transefected 293T cells detected by RT-qPCR and western blotting,

indicating effective knockdown of STIL in Lv-shSTIL group could effectively down regulate STIL expression at mRNA and protein levels in lung adenocarcinoma cells. **p<0.01, Compared with Lv-shCtrl group.

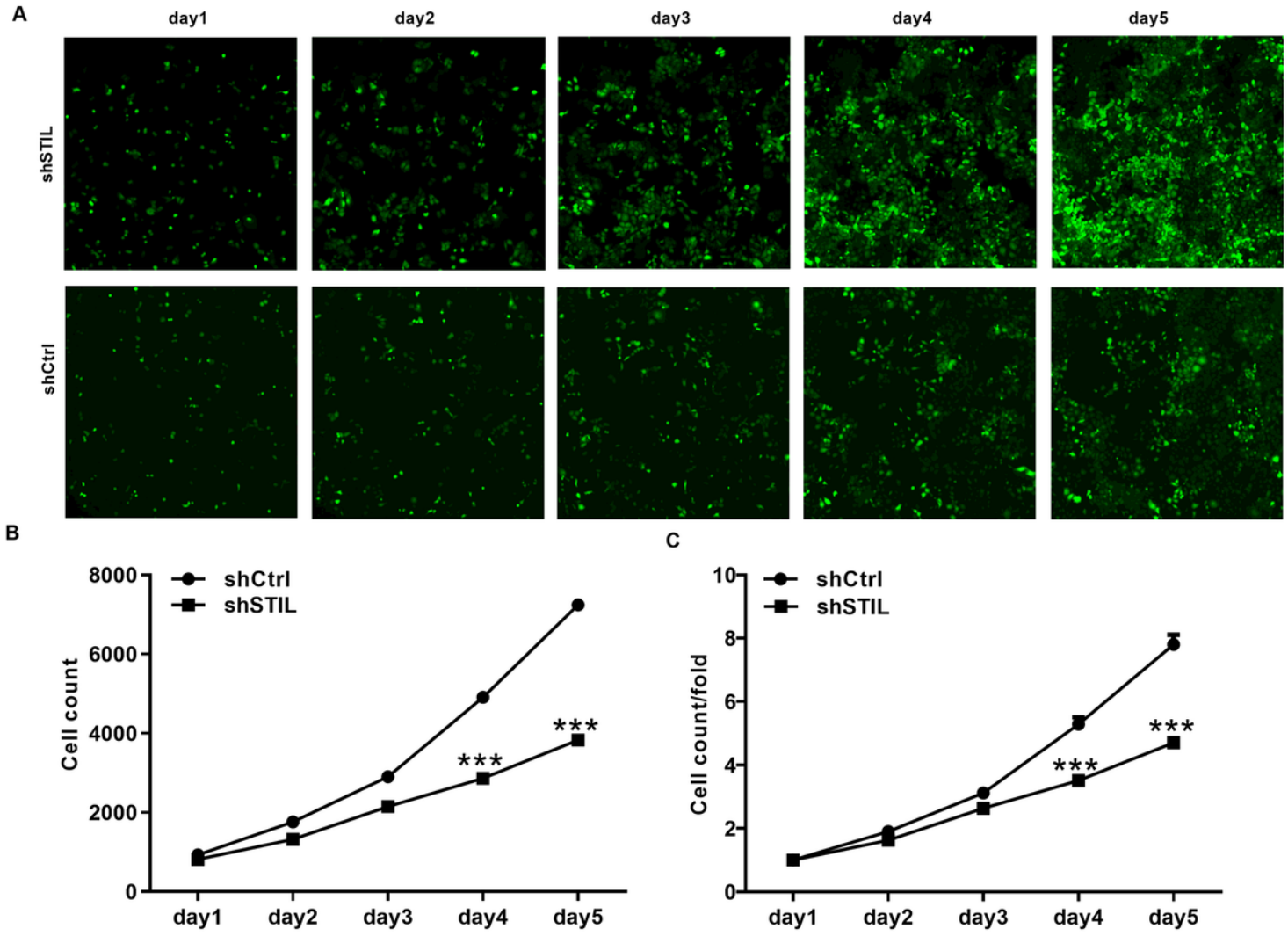

Figure 3

(A, B): Effect of STIL gene knockdown on cell proliferation by Cellomics Array Scan VTI imaging detection. The detection result of GFP-based Cellomics Array Scan VTI imaging assay showed the number of cells and the fold-change of proliferation were markedly reduced in the STIL-shRNA-silenced lung adenocarcinoma cells on the third, fourth and fifth day following STIL silenced significantly in NCI-H1299 cells compared with that of Lv-shCtrl group, as shown in Figure 3(A, B). Therefore, it is suggested that silencing of STIL could inhibit lung adenocarcinoma cell proliferation. ***P<0.001, Compared with Lv-shCtrl group.

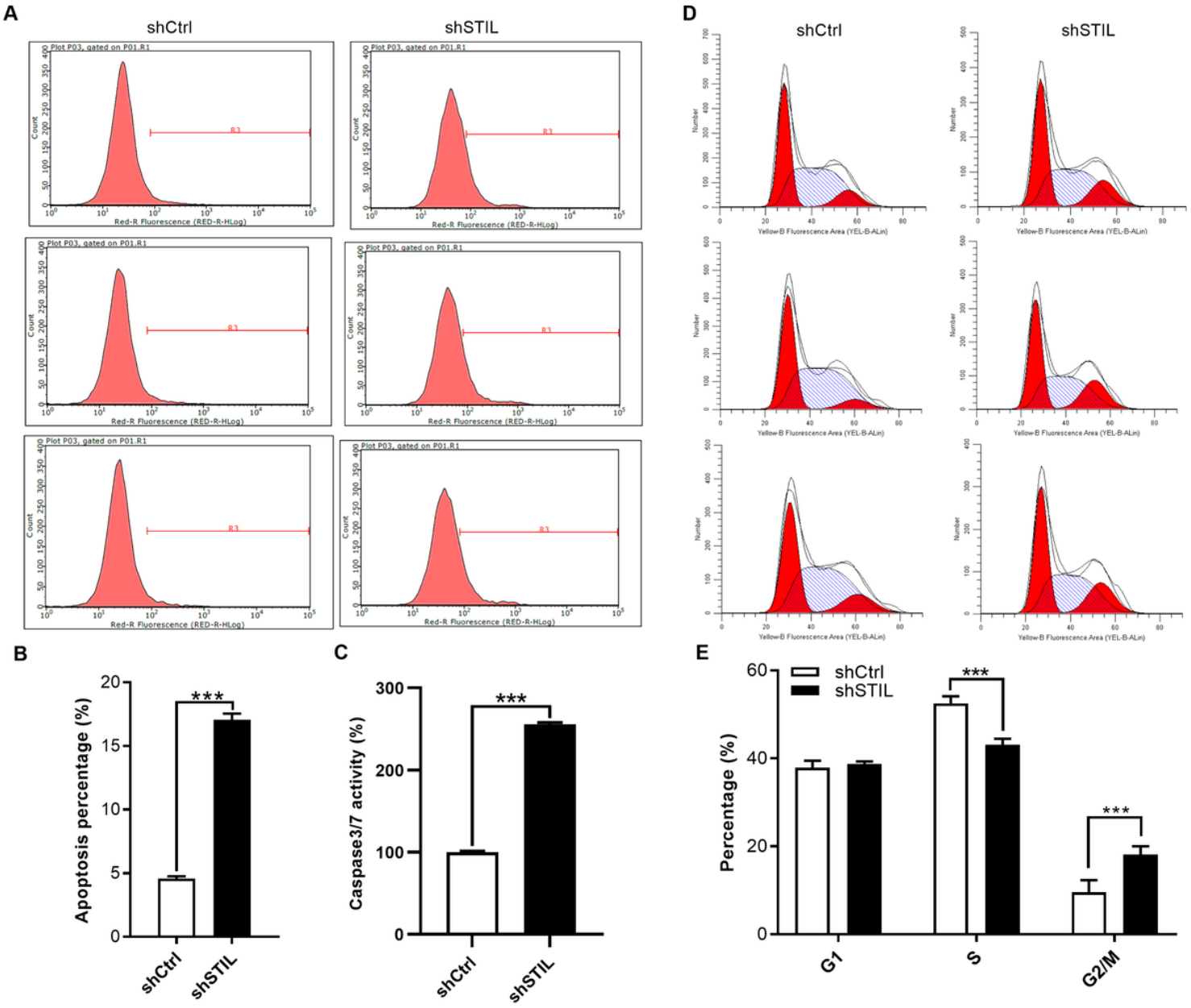

Figure 4

(A, B): Effect of STIL gene knockdown on apoptosis and cell cycle. After infection with shRNA lentivirus and its negative control lentivirus for 5 days, the apoptotic NCI-H1299 cells in Lv-shSTIL infection group increased significantly with the comparison of that in Lv-shCtrl group ($p < 0.001$), suggesting that silencing of STIL could induce apoptosis of lung adenocarcinoma cell NCI-H1299 cells. Compared with Lv-shCtrl group.The caspase 3/7 activity of the Lv-shSTIL group was calculated based on the Lv-shCtrl group. Compared with Lv-shCtrl group, caspase 3/7 activity increased in Lv-shSTIL group, indicating that the number of apoptotic cells increased compared with Lv-shCtrl group. The cell cycle was assessed between STIL silenced NCI-H1299 cells and shCtrl group cells by flow cytometry using PI (Sigma, USA). Three days after shRNA lentivirus infection, there was no significant difference in G1 cells in the experimental group. The number of NCI-H1299-silenced cells in S phase decreased, and the number of cells in G2/M phase increased than that in shCtrl group cells ($P<0.05$). These data suggested that silencing of STIL could arrest cell cycle in G2 phase, as shown in Figure 7(A, B). ***$P<0.001$, Compared with Lv-shCtrl group.

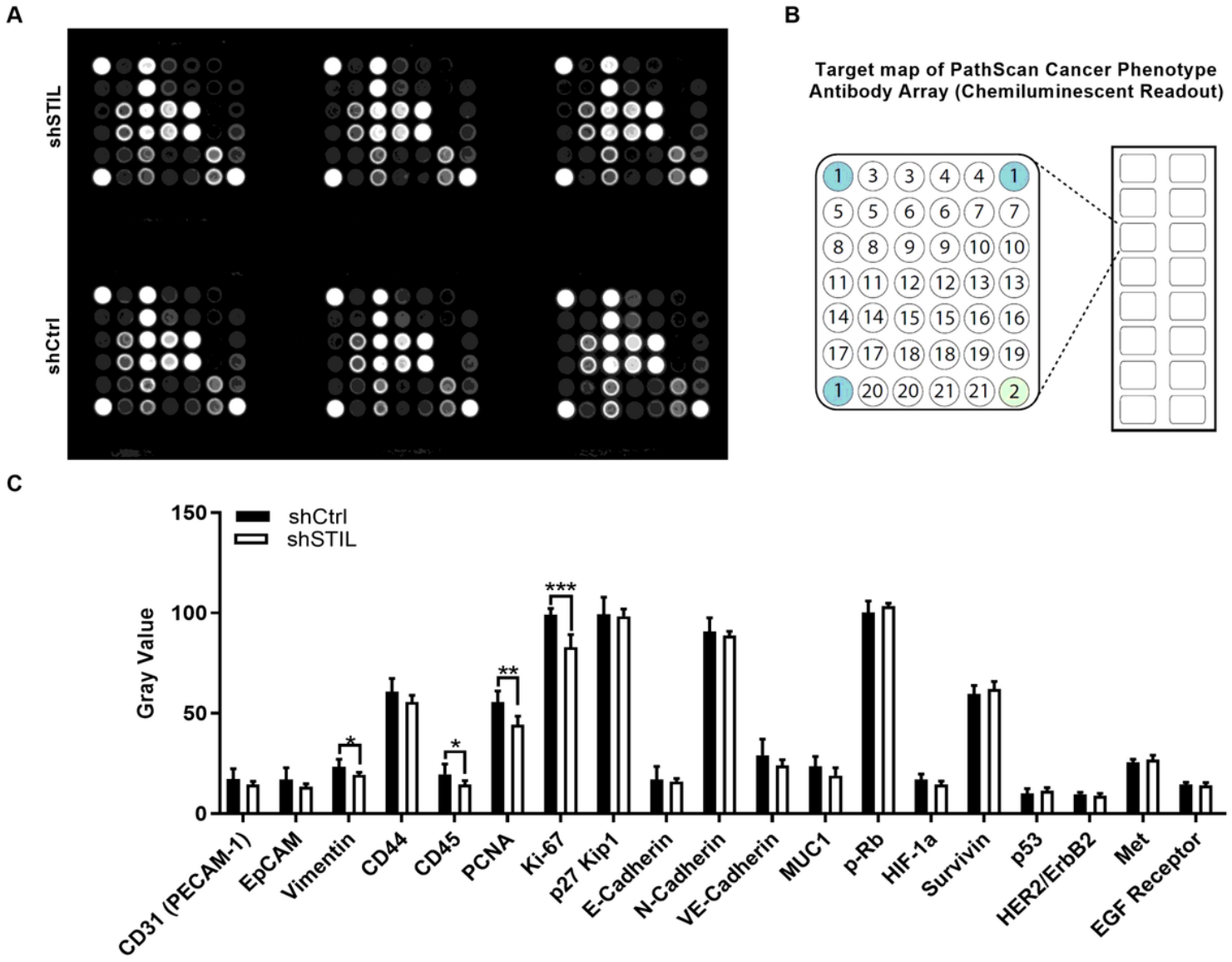

Figure 5

(A, B, C): Effects of STIL gene knockdown on relevant targets of cancer phenotype array in NCI-H1299 cells. After STIL gene was knockdown successfully in NCI-H1299 cells, PathScan RTK Signaling pathway Antibody Array was used to explore aberrantly expressed proteins between Lv-shSTIL-infected cells and Lv-shCtrl-infected cells. The results showed that knockdown of STIL could significantly induce downregulation of protein expressions of Vimentin、CD45、PCNA and Ki-67 at the levels about -17.19%, -26.43%, -20.46% and -16.36%, respectively (p value= 0.0416, 0.0430, 0.0024 and 0.0002), as shown in Figure 8(A, B). ***P<0.001, Compared with Lv-shCtrl group.

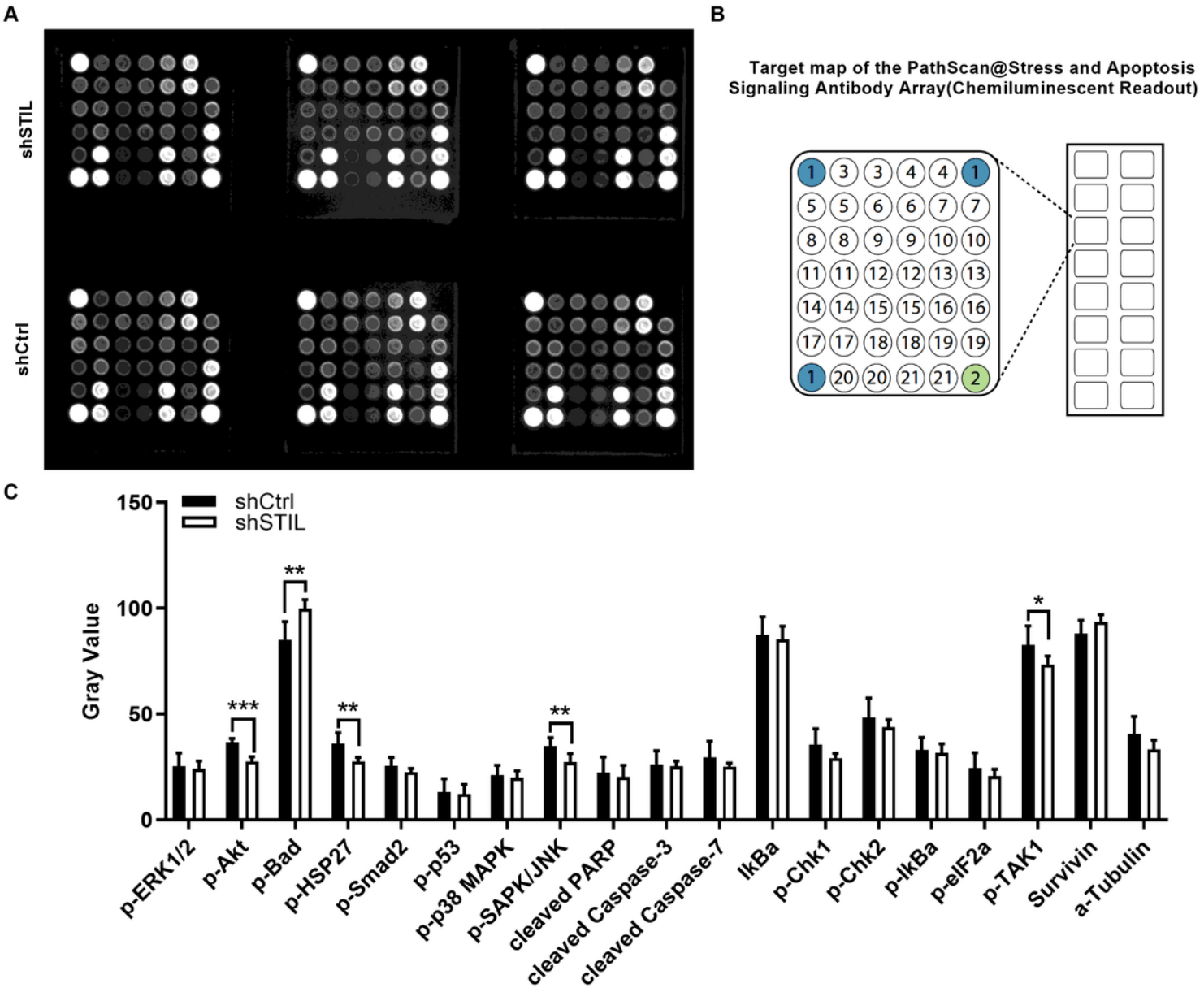

Figure 6

(A, B, C): Effects of STIL gene knockdown on relevant targets of stress and apoptosis signaling pathway in NCI-H1299 cells. After STIL gene was knockdown successfully in NCI-H1299 cells, PathScan stress and apoptosis pathway Antibody Array was used to explore aberrantly expressed proteins between Lv-shSTIL-infected cells and Lv-shCtrl-infected cells. The results showed that knockdown of STIL could significantly induce downregulation of phosphorylation expressions of p-Akt、p-Bad、p-HSP27、p-SAPK/JNK and p-TAK1 at the level about -17.14%, -22.54%, -13.43%, -23.18%, -23.18%. -14.33% and -29.02%, respectively (p value=0.0000, 0.0038, 0.0027, 0.0079 and 0.0458). ***P<0.001, Compared with Lv-shCtrl group.